



Supplement of

Measurement report: Formation of tropospheric brown carbon in a lifting air mass

Can Wu et al.

Correspondence to: Si Zhang (szhang@geo.ecnu.edu.cn) and Gehui Wang (ghwang@geo.ecnu.edu.cn)

The copyright of individual parts of the supplement might differ from the article licence.

1 **S1. UV–vis light absorption measurement**

2 About 8 punches (12 cm³) from each filter sample was extracted three times under sonication
3 with 15 ml Milli-Q pure water (18.2 MΩ), and the extract was subsequently filtered through
4 0.45 μm PTFE pore syringe filter to remove the insoluble component in the suspension. A
5 liquid waveguide capillary UV–vis spectrometer equipped with a 1 m long-effective path
6 detection cell was applied to record the light absorption spectra of all extracts. The light
7 absorption spectrum was finally converted into absorption coefficient (*abs*_λ, M/m) at a
8 particular wavelength (λ) using the following equation.

Eq.S1

$$abs_{\lambda} = (A_{\lambda} - A_{700}) \frac{v_1}{v_a \times l} \times \ln(10)$$

9 Where *A*_λ and *A*₇₀₀ represent the light absorption of the extracts at wavelength λ and 700 nm,
10 respectively. *V*₁ corresponds to the volume of the extract, e.g., 15 ml; *V*_a refers to the volume of
11 the air through corresponding to filter punches; *l* (m) is the absorbing path length. While, ln(10)
12 is used for converting common logarithm that provided by the spectrophotometer to natural
13 logarithm.

14
15
16
17
18
19
20

21
22
23

Table S1 The result of bootstrap analysis.

Sources	Secondary formation	Fossil fuel combustion	Biomass burning	Fugitive dust	Unmapped
Secondary formation	50	0	0	0	0
Fossil fuel combustion	1	49	0	0	0
Biomass burning	0	0	50	0	0
Fugitive dust	0	5	0	45	0

24
25
26
27
28

Table S2 RF model performance for testing dataset.

	MF site	MS site
R ²	0.92	0.86
MSE	0.003	0.008
RMSE	0.054	0.091
MAE	0.04	0.07

30 Note: MSE: mean square error; RMSE: root-mean-square error; MAE: mean absolute error.

31
32
33
34

Table S3. Information and mass concentration ($\mu\text{g m}^{-3}$) of nitroaromatic compounds detected in this study.

Compounds	Molecular weight	Formula	CAS number	Abbreviation	MF site	MS site
4-Nitrophenol	139.11	C ₆ H ₅ NO ₃	100-02-7	4NP	2.6±2.6	0.40±0.25
3-Methoxy-4-nitrophenol	153.14	C ₇ H ₇ NO ₃	2581-34-2	3M4NP	0.07±0.05	0.01±0.01
4-Nitrocatechol	155.11	C ₆ H ₅ NO ₄	59030-13-6	4NC	1.6±2.5	0.25±0.67
4-Methyl-5-nitrocatechol	169.13	C ₇ H ₇ NO ₄	68906-21-8	4M5NC	11.4±11.4	1.8±1.3
3-Nitrosalicylic acid	183.12	C ₇ H ₅ NO ₅	85038-1	3NSA	0.01±0.01	0.004±0.01
5-Nitrosalicylic acid	183.12	C ₇ H ₅ NO ₅	96-97-9	5NSA	0.13±0.13	0.012±0.015

37
38
39
40
41
42
43

44
45
46

Table S4 NH₃ concentrations in different regions of China

Region	Location	Period	Ammonia ($\mu\text{g m}^{-3}$)	Reference
NCP	Beijing	Summer of 2009	29.4±11.9	Meng et al. (2017)
		Mar.2016-May.2017	22.2±12.8	Kuang et al. (2020)
	Gucheng	May-Sep 2013	27.5±42.8	Meng et al. (2018)
	Luancheng	Dec.2015-Feb.2016	17.2	Pan et al. (2018)
Cangzhou	Dec.2015-Feb.2016	22.2		
FWP	Xi'an	Winter of 2016	29±7.3	Wu et al. (2020a)
		Summer of 2016	38±9.4	
	Weinan	2006-2007	12.9	Cao et al. (2009)
		Dec.2015-Feb.2016	12.4	Pan et al. (2018)
		Summer of 2020	3.1±1.9	Wu et al. (2022)
Mt. Hua-MF	Summer of 2020	27.3±51		
YRD		Autumn of 2019	9.5	Wu et al. (2023)
		July-Dec 2013, Mar-June 2014	9.4±6.9	Wang et al. (2015)
	Shanghai	Dec.2019-Jan.2020	9.3±4.0	Lv et al. (2022)
	Nanjing	Dec.2015-Feb.2016	10.8	Pan et al. (2018)
	Taihu	Dec.2015-Feb.2016	6.3	
	Lin'an	Sep 2009-Dec 2010	12.5±8.5	Meng et al. (2014)
PRD	Guangzhou	Dec.2015-Feb.2016	5.8	Pan et al. (2018)
		Oct-Nov 2004	7.3±6.2	Hu et al. (2008)
	Dinghushan	Dec.2015-Feb.2016	2.8	Pan et al. (2018)
	Maoming	Dec.2015-Feb.2016	9.8	
Hongkong	Autumn 2000	2.3±2.7	Yao et al. (2006)	
TP	Lhasa	Dec.2015-Feb.2016	4.8	Pan et al. (2018)
	Ali	Dec.2015-Feb.2016	1.7	

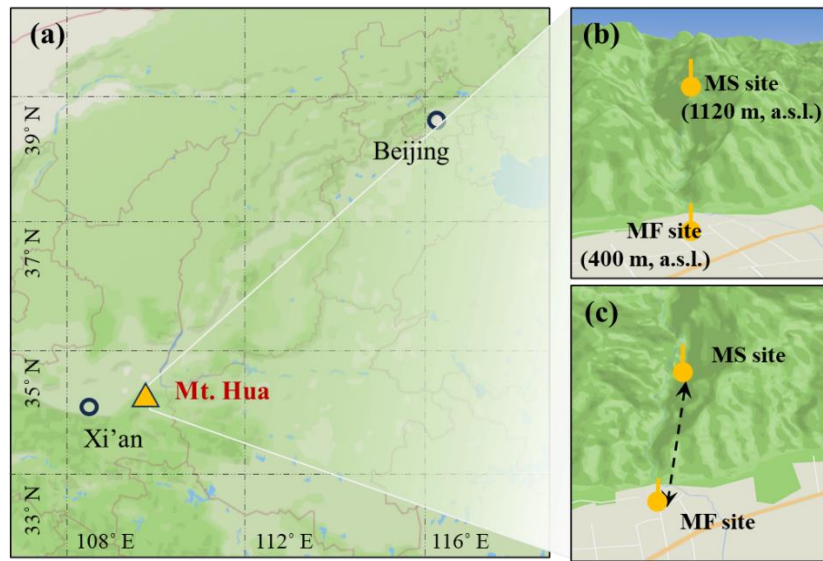
47 Note: In some cities, the NH₃ unit is ppb, which was converted by the formula of standard atmospheric
48 pressure and normal temperature in this study. The abbreviations of NCP, FWP, YRD, PRD and TP indicate
49 North China Plain, Fen-wei Plain, Yangtze River Delta, Pearl River Delta and Tibet Plateau, respectively.

50
51
52

53 **Table S5** MAE₃₆₅ of water-soluble BrC in PM_{2.5} among different cities in the world.

Region	Location	Year	Season	MAE ₃₆₅ (m ² g ⁻¹)	Reference
NCP, China	Beijing	2011	Winter	1.2±0.1	Cheng et al. (2016)
		2010-2011	Winter	1.26	Du et al. (2014)
		2010-2011	Summer	0.51	
	Xingtai	2018-2019	Spring	1.4±0.18	Li et al. (2023a)
			Summer	0.95±0.18	
		Autumn	1.5±0.13		
		Winter	1.9±0.16		
	Jinan (TSP)	2016	Spring	1.00±0.23	Wen et al. (2021)
	Zhangbei	2016	Spring	1.32±0.34	
	Tianjin	2016–2017	Winter	1.54±0.33	Deng et al. (2022)
Summer			0.84±0.22		
FWP, China	Xi'an	2016–2017	Winter	1.2±0.06	Wu et al. (2020b)
		Summer	1.1±0.2	Li et al. (2023b)	
	2020	Winter	0.78 ± 0.96		
	Licun	2017	Winter	0.94±0.28	Li et al. (2020)
			Summer	1.01±0.18	
	Mt. Hua-MS	2016	Summer	0.69±0.2	This study
Mt. Hua-MF	0.67±0.21				
YRD, China	Changzhou	2018	Winter	0.74	Tao et al. (2021)
	Yangzhou	2015-2016	Annual	0.75 ± 0.29	Chen et al. (2020)
			Spring	0.69	
			Summer	0.51	
	Nanjing	2015-2016	Autumn	0.55	Chen et al. (2018)
			Winter	1.04	
Shanghai	2018-2019	Winter	1.18±0.42	Zhao et al. (2021)	
PRD, China	Guangzhou	2012	Winter	0.81	Liu et al. (2018)
		2018	Winter	1.0 ± 0.21	Zou et al. (2023)
		2019	Winter	0.34	Wang et al. (2022)
		2016	Autumn	0.60±0.06	He et al. (2023)
	Taipei	2021	Annual	0.86±0.60	Ting et al. (2022)
TP, China	Lulang	2015-2016	Winter	0.75 ± 0.13	Zhu et al. (2018)
	Lhasa	2013-2014	Annual	0.74	Li et al. (2016)
			Summer	0.27 ± 0.10	
	Southeast TP	2013-2014	Winter	0.86 ± 0.17	Wu et al. (2020c)
			Summer	0.38±0.16	
Nam Co	2015	Summer	0.38±0.16	Zhang et al. (2017)	
India	Delhi	2016	Spring	2.5	Dasari et al. (2019)
Korea	Seoul	2012-2013	Winter	1.02	Kim et al. (2016)
			Summer	0.28	
USA	Los Angeles	2018-2019	Winter	0.7±0.2	Soleimanian et al. (2020)
			Summer	0.5±0.2	
	Yorkville	2010	Winter	0.41	Hecobian et al. (2010)
Switzerland		2013	Summer	0.29	Xie et al. (2019)
			Winter	0.9	
Greece	Ioannina	2019	Summer	0.3 ± 0.1	Paraskevopoulou et al. (2023)
			Summer	0.28	

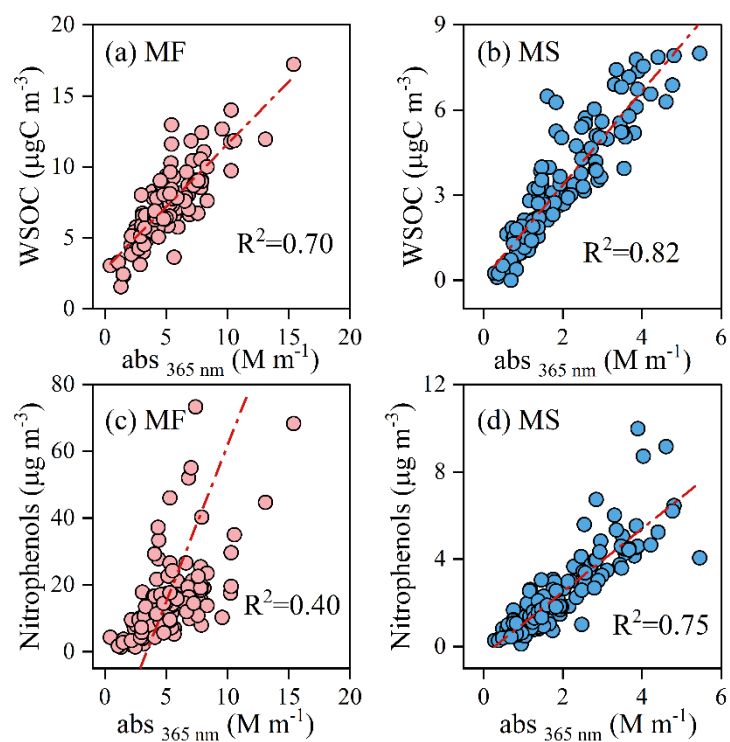
55
56
57
58
59
60
61
62
63



64
65
66
67
68
69

Figure S1. Locations of the sampling sites in China. **(a)** Topographic view, **(b)** vertical view and bird's-eye view **(c)** of Mt. Hua with the sampling sites marked. The maps are the reproductions from ©Mapbox (<https://account.mapbox.com/>, last access: 16 March 2024)

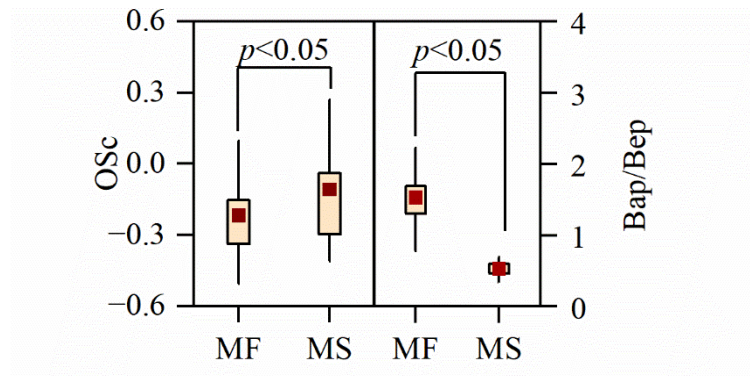
70
71
72



73
74
75
76
77
78

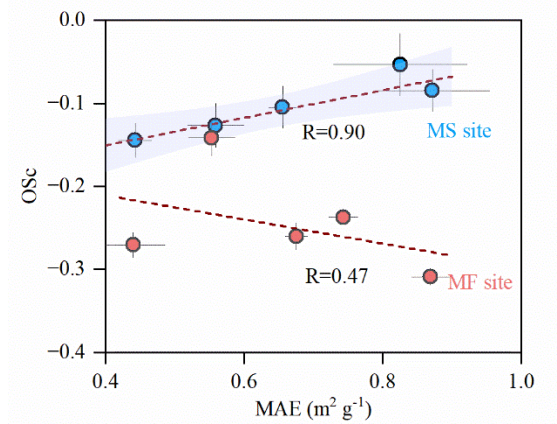
Figure S2. Linear fit regression analysis for Abs_{λ=365 nm} with WSOC and nitrophenols at MF and MS sites

79
80



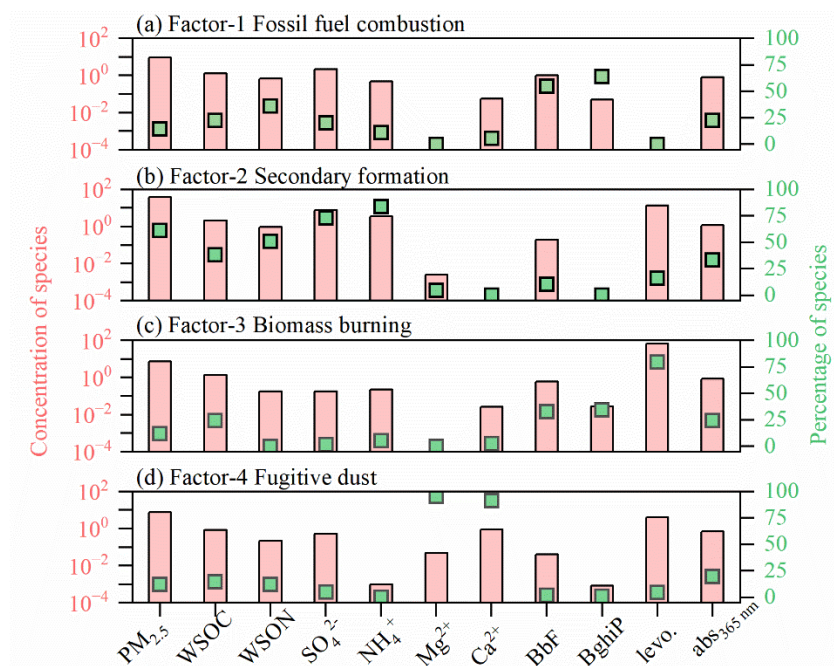
81
82
83
84
85
86

Figure S3 Comparison of OSc and BaP/BeP ratio among both sampling sites. The whisker boxes show mean (square), 25th–75th percentile ranges (box), and standard deviation values (whiskers)



87
88
89
90
91
92
93

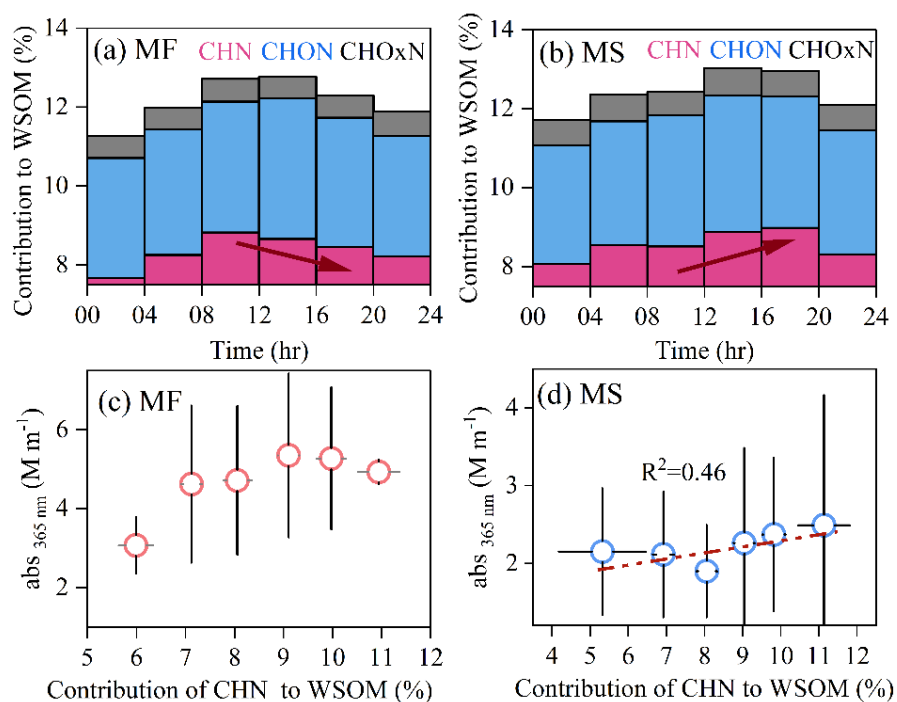
Figure S4. The correlativity between MAE_{365nm} and OSc value at both sampling sites.



94
95
96
97
98

Figure S5. Source apportionment for light absorption of daytime water-soluble BrC ($abs_{365\text{ nm}}$) of all the daytime samples collected during the whole campaign.

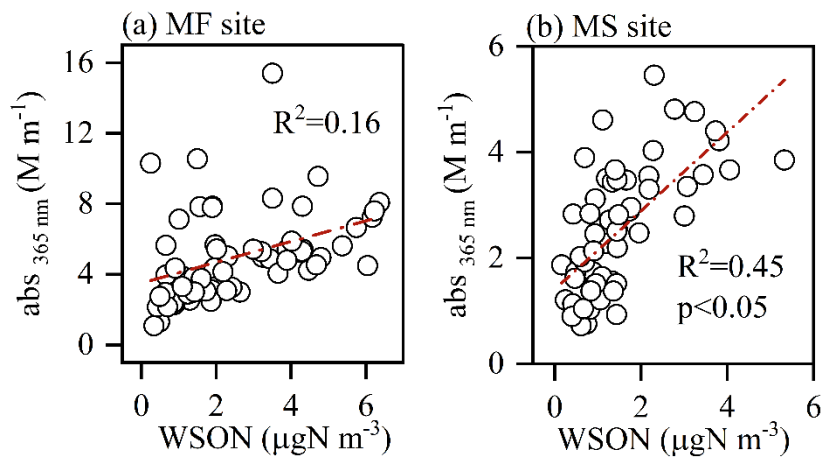
99
100
101



102
103
104
105
106
107
108
109
110

Figure S6. (a) and (b) Diurnal variations in relative contributions of nitrogen-containing organic fragments to WSOM at MF and MS sites, respectively. (c and d) The dependence of light absorption of WSOC ($\text{Abs}_{\lambda=365 \text{ nm}}$) on the relative contributions of CHN fragments to WSOM at the two sampling sites.

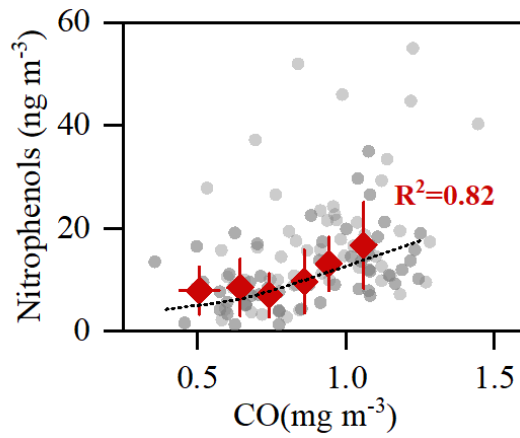
111
112
113
114
115
116
117



118
119
120

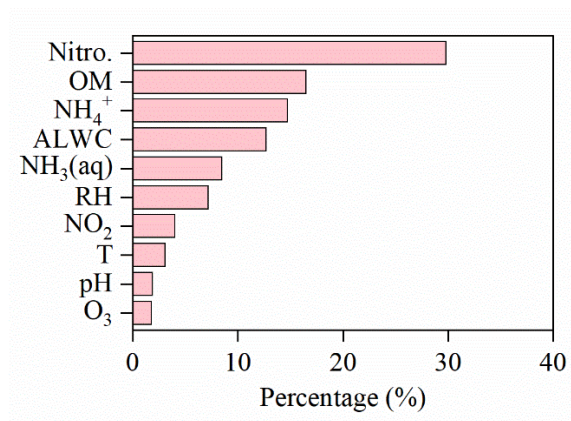
Figure S7 Linear fit regression analysis for $\text{Abs}_{\lambda=365 \text{ nm}}$ and WSON of the daytime samples at two sites

121
122
123
124
125
126
127
128
129
130



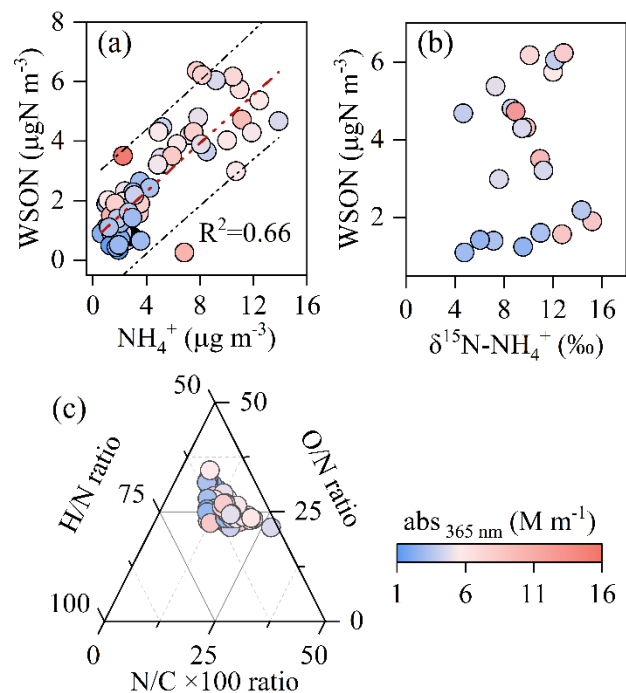
131
132
133
134
135
136
137

Figure S8 A correlation analysis of CO and NACs at MF site.



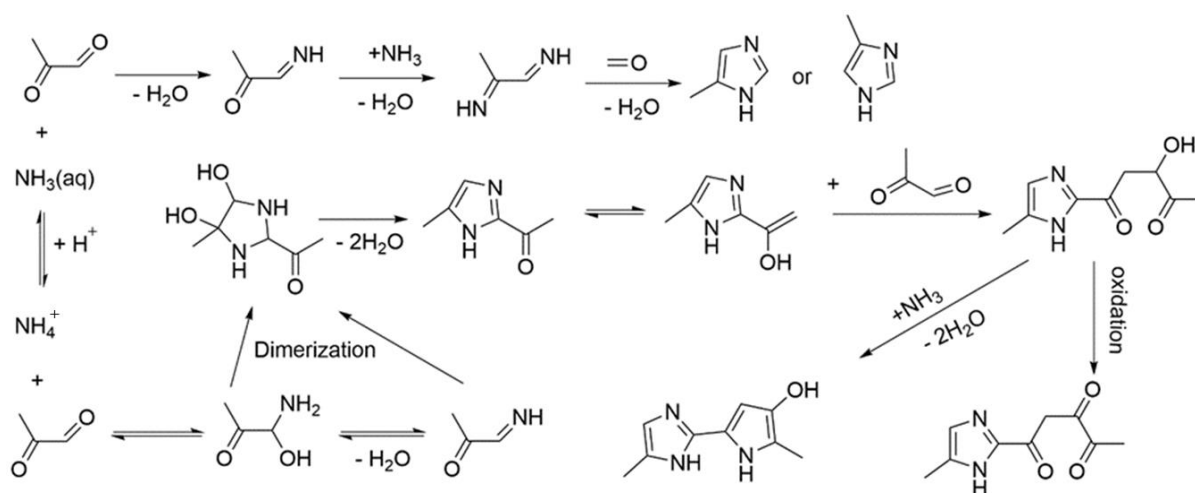
138
139
140
141
142

Figure S9 Importance assessment for the key factors affecting the daytime WSON at MF site.



143
 144
 145
 146
 147
 148
 149
 150

Figure S10 Impacts on WSON formation at MF site. Linear fit regressions for WSON with $\text{NH}_4^+ + \text{NH}_3(\text{aq})$ (a) and $\delta^{15}\text{N-NH}_4^+$ (b) at MF site and triangular chart for the elemental ratios of N/C, H/N and O/N of WSOC at MF site (c).



151
 152
 153
 154

Figure S11 Simple reaction paths for imidazoles or N-heterocycles (Modified from Aiona et al. (2017) and Jang et al. (2013)).

155

References

- 156 Aiona, P. K., Lee, H. J., Leslie, R., Lin, P., Laskin, A., Laskin, J., and Nizkorodov, S. A.: Photochemistry of
 157 Products of the Aqueous Reaction of Methylglyoxal with Ammonium Sulfate, *ACS Earth Space Chem.*, 1,
 158 522-532, 10.1021/acsearthspacechem.7b00075, 2017.
- 159 Cao, J.-J., Zhang, T., Chow, J. C., Watson, J. G., Wu, F., and Li, H.: Characterization of Atmospheric Ammonia
 160 over Xi'an, China, *Aerosol Air Qual. Res.*, 9, 277-289, 2009.
- 161 Chen, Y., Ge, X., Chen, H., Xie, X., Chen, Y., Wang, J., Ye, Z., Bao, M., Zhang, Y., and Chen, M.: Seasonal light
 162 absorption properties of water-soluble brown carbon in atmospheric fine particles in Nanjing, China, *Atmos.*
 163 *Environ.*, 187, 230-240, 10.1016/j.atmosenv.2018.06.002, 2018.
- 164 Chen, Y., Xie, X., Shi, Z., Li, Y., Gai, X., Wang, J., Li, H., Wu, Y., Zhao, X., Chen, M., and Ge, X.: Brown carbon
 165 in atmospheric fine particles in Yangzhou, China: Light absorption properties and source apportionment,
 166 *Atmos. Res.*, 244, 10.1016/j.atmosres.2020.105028, 2020.
- 167 Cheng, Y., He, K.-b., Du, Z.-y., Engling, G., Liu, J.-m., Ma, Y.-l., Zheng, M., and Weber, R. J.: The characteristics
 168 of brown carbon aerosol during winter in Beijing, *Atmos. Environ.*, 127, 355-364,
 169 10.1016/j.atmosenv.2015.12.035, 2016.
- 170 Dasari, S., Andersson, A., Bikkina, S., Holmstrand, H., Budhavant, K., Satheesh, S., Asmi, E., Kesti, J., Backman,
 171 J., Salam, A., Bisht, D. S., Tiwari, S., Hameed, Z., and Gustafsson, O.: Photochemical degradation affects the
 172 light absorption of water-soluble brown carbon in the South Asian outflow, *Science Advances*, 5,
 173 10.1126/sciadv.aau8066, 2019.
- 174 Deng, J., Ma, H., Wang, X., Zhong, S., Zhang, Z., Zhu, J., Fan, Y., Hu, W., Wu, L., Li, X., Ren, L., Pavuluri, C. M.,
 175 Pan, X., Sun, Y., Wang, Z., Kawamura, K., and Fu, P.: Measurement report: Optical properties and sources of
 176 water-soluble brown carbon in Tianjin, North China insights from organic molecular compositions, *Atmos.*
 177 *Chem. Phys.*, 22, 6449-6470, 10.5194/acp-22-6449-2022, 2022.
- 178 Du, Z., He, K., Cheng, Y., Duan, F., Ma, Y., Liu, J., Zhang, X., Zheng, M., and Weber, R.: A yearlong study of
 179 water-soluble organic carbon in Beijing II: Light absorption properties, *Atmospheric Environment*, 89, 235-
 180 241, 2014.
- 181 He, T., Wu, Y., Wang, D., Cai, J., Song, J., Yu, Z., Zeng, X., and Peng, P. a.: Molecular compositions and optical
 182 properties of water-soluble brown carbon during the autumn and winter in Guangzhou, China, *Atmos.*
 183 *Environ.*, 296, 10.1016/j.atmosenv.2022.119573, 2023.
- 184 Hecobian, A., Zhang, X., Zheng, M., Frank, N., Edgerton, E. S., and Weber, R. J.: Water-Soluble Organic Aerosol
 185 material and the light-absorption characteristics of aqueous extracts measured over the Southeastern United
 186 States, *Atmos. Chem. Phys.*, 10, 5965-5977, 10.5194/acp-10-5965-2010, 2010.
- 187 Hu, M., Wu, Z., Slanina, J., Lin, P., Liu, S., and Zeng, L.: Acidic gases, ammonia and water-soluble ions in PM_{2.5}
 188 at a coastal site in the Pearl River Delta, China, *Atmos. Environ.*, 42, 6310-6320,
 189 10.1016/j.atmosenv.2008.02.015, 2008.
- 190 Jang, H. W., Jiang, Y., Hengel, M., and Shibamoto, T.: Formation of 4(5)-Methylimidazole and Its Precursors, α -
 191 Dicarbonyl Compounds, in *Maillard Model Systems*, *J. Agric. Food. Chem.*, 61, 6865-6872,
 192 10.1021/jf401958w, 2013.
- 193 Kim, H., Kim, J. Y., Jin, H. C., Lee, J. Y., and Lee, S. P.: Seasonal variations in the light-absorbing properties of
 194 water-soluble and insoluble organic aerosols in Seoul, Korea, *Atmos. Environ.*, 129, 234-242,
 195 10.1016/j.atmosenv.2016.01.042, 2016.
- 196 Kuang, Y., Xu, W., Lin, W., Meng, Z., Zhao, H., Ren, S., Zhang, G., Liang, L., and Xu, X.: Explosive morning
 197 growth phenomena of NH₃ on the North China Plain: Causes and potential impacts on aerosol formation,
 198 *Environ. Pollut.*, 257, 10.1016/j.envpol.2019.113621, 2020.

199 Li, C., Chen, P., Kang, S., Yan, F., Hu, Z., Qu, B., and Sillanpaa, M.: Concentrations and light absorption
200 characteristics of carbonaceous aerosol in PM_{2.5} and PM₁₀ of Lhasa city, the Tibetan Plateau, *Atmos.*
201 *Environ.*, 127, 340-346, 10.1016/j.atmosenv.2015.12.059, 2016.

202 Li, D., Wu, C., Zhang, S., Lei, Y., Lv, S., Du, W., Liu, S., Zhang, F., Liu, X., Liu, L., Meng, J., Wang, Y., Gao, J.,
203 and Wang, G.: Significant coal combustion contribution to water-soluble brown carbon during winter in
204 Xingtai, China: Optical properties and sources, *J. Environ. Sci.*, 124, 892-900, 10.1016/j.jes.2022.02.026,
205 2023a.

206 Li, J., Zhang, Q., Wang, G., Li, J., Wu, C., Liu, L., Wang, J., Jiang, W., Li, L., Ho, K. F., and Cao, J.: Optical
207 properties and molecular compositions of water-soluble and water-insoluble brown carbon (BrC) aerosols in
208 northwest China, *Atmos. Chem. Phys.*, 20, 4889-4904, 10.5194/acp-20-4889-2020, 2020.

209 Li, X., Yu, F., Song, Y., Zhang, C., Yan, F., Hu, Z., Lei, Y., Tripathee, L., Zhang, R., Guo, J., Wang, Y., Chen, Q.,
210 Liu, L., Cao, J., and Wang, Q.: Water-soluble brown carbon in PM_{2.5} at two typical sites in Guanzhong Basin:
211 Optical properties, sources, and implications, *Atmos. Res.*, 281, 10.1016/j.atmosres.2022.106499, 2023b.

212 Liu, J., Mo, Y., Ding, P., Li, J., Shen, C., and Zhang, G.: Dual carbon isotopes (C-14 and C-13) and optical
213 properties of WSOC and HULIS-C during winter in Guangzhou, China, *Sci. Total Environ.*, 633, 1571-1578,
214 10.1016/j.scitotenv.2018.03.293, 2018.

215 Lv, S., Wang, F., Wu, C., Chen, Y., Liu, S., Zhang, S., Li, D., Du, W., Zhang, F., Wang, H., Huang, C., Fu, Q.,
216 Duan, Y., and Wang, G.: Gas-to-Aerosol Phase Partitioning of Atmospheric Water-Soluble Organic
217 Compounds at a Rural Site in China: An Enhancing Effect of NH₃ on SOA Formation, *Environ. Sci. Technol.*,
218 56, 3915-3924, 10.1021/acs.est.1c06855, 2022.

219 Meng, Z., Lin, W., Zhang, R., Han, Z., and Jia, X.: Summertime ambient ammonia and its effects on ammonium
220 aerosol in urban Beijing, China, *Sci. Total Environ.*, 579, 1521-1530, 10.1016/j.scitotenv.2016.11.159, 2017.

221 Meng, Z., Zhang, R., Lin, W., Jia, X., Yu, X., Yu, X., and Wang, G.: Seasonal Variation of Ammonia and
222 Ammonium Aerosol at a Background Station in the Yangtze River Delta Region, China, *Aerosol Air Qual.*
223 *Res.*, 14, 756-766, 10.4209/aaqr.2013.02.0046, 2014.

224 Meng, Z., Xu, X., Lin, W., Ge, B., Xie, Y., Song, B., Jia, S., Zhang, R., Peng, W., Wang, Y., Cheng, H., Yang, W.,
225 and Zhao, H.: Role of ambient ammonia in particulate ammonium formation at a rural site in the North China
226 Plain, *Atmos. Chem. Phys.*, 18, 167-184, 10.5194/acp-18-167-2018, 2018.

227 Moschos, V., Kumar, N. K., Daellenbach, K. R., Baltensperger, U., Prevot, A. S. H., and El Haddad, I.: Source
228 Apportionment of Brown Carbon Absorption by Coupling Ultraviolet-Visible Spectroscopy with Aerosol
229 Mass Spectrometry, *Environmental Science & Technology Letters*, 5, 302-+, 10.1021/acs.estlett.8b00118,
230 2018.

231 Pan, Y., Tian, S., Zhao, Y., Zhang, L., Zhu, X., Gao, J., Huang, W., Zhou, Y., Song, Y., Zhang, Q., and Wang, Y.:
232 Identifying Ammonia Hotspots in China Using a National Observation Network, *Environ. Sci. Technol.*, 52,
233 3926-3934, 10.1021/acs.est.7b05235, 2018.

234 Paraskevopoulou, D., Kaskaoutis, D. G., Grivas, G., Bikkina, S., Tsagkaraki, M., Vrettou, I. M., Tavernaraki, K.,
235 Papoutsidaki, K., Stavroulas, I., Liakakou, E., Bougiatioti, A., Oikonomou, K., Gerasopoulos, E., and
236 Mihalopoulos, N.: Brown carbon absorption and radiative effects under intense residential wood burning
237 conditions in Southeastern Europe: New insights into the abundance and absorptivity of methanol-soluble
238 organic aerosols, *Sci. Total Environ.*, 860, 10.1016/j.scitotenv.2022.160434, 2023.

239 Soleimanian, E., Mousavi, A., Taghvaei, S., Shafer, M. M., and Sioutas, C.: Impact of secondary and primary
240 particulate matter (PM) sources on the enhanced light absorption by brown carbon (BrC) particles in central
241 Los Angeles, *Sci. Total Environ.*, 705, 10.1016/j.scitotenv.2019.135902, 2020.

242 Tao, Y., Sun, N., Li, X., Zhao, Z., Ma, S., Huang, H., Ye, Z., and Ge, X.: Chemical and Optical Characteristics and

243 Sources of PM_{2.5} Humic-Like Substances at Industrial and Suburban Sites in Changzhou, China,
 244 Atmosphere, 12, 10.3390/atmos12020276, 2021.

245 Ting, Y.-C., Ko, Y.-R., Huang, C.-H., Cheng, Y.-H., and Huang, C.-H.: Optical properties and potential sources of
 246 water-soluble and methanol-soluble organic aerosols in Taipei, Taiwan, Atmos. Environ., 290,
 247 10.1016/j.atmosenv.2022.119364, 2022.

248 Wang, D., Shen, Z., Zhang, Q., Lei, Y., Zhang, T., Huang, S., Sun, J., Xu, H., and Cao, J.: Winter brown carbon
 249 over six of China's megacities: light absorption, molecular characterization, and improved source
 250 apportionment revealed by multilayer perceptron neural network, Atmos. Chem. Phys., 22, 14893-14904,
 251 10.5194/acp-22-14893-2022, 2022.

252 Wang, S., Nan, J., Shi, C., Fu, Q., Gao, S., Wang, D., Cui, H., Saiz-Lopez, A., and Zhou, B.: Atmospheric
 253 ammonia and its impacts on regional air quality over the megacity of Shanghai, China, Sci. Rep., 5,
 254 10.1038/srep15842, 2015.

255 Wen, H., Zhou, Y., Xu, X., Wang, T., Chen, Q., Chen, Q., Li, W., Wang, Z., Huang, Z., Zhou, T., Shi, J., Bi, J., Ji,
 256 M., and Wang, X.: Water-soluble brown carbon in atmospheric aerosols along the transport pathway of Asian
 257 dust: Optical properties, chemical compositions, and potential sources, Sci. Total Environ., 789,
 258 10.1016/j.scitotenv.2021.147971, 2021.

259 Wu, C., Cao, C., Li, J., Lv, S., Li, J., Liu, X., Zhang, S., Liu, S., Zhang, F., Meng, J., and Wang, G.: Different
 260 physicochemical behaviors of nitrate and ammonium during transport: a case study on Mt. Hua, China, Atmos.
 261 Chem. Phys., 22, 15621-15635, 10.5194/acp-22-15621-2022, 2022.

262 Wu, C., Wang, G., Li, J., Li, J., Cao, C., Ge, S., Xie, Y., Chen, J., Liu, S., Du, W., Zhao, Z., and Cao, F.: Non-
 263 agricultural sources dominate the atmospheric NH₃ in Xi'an, a megacity in the semi-arid region of China, Sci.
 264 Total Environ., 722, 137756, 10.1016/j.scitotenv.2020.137756, 2020a.

265 Wu, C., Lv, S., Wang, F., Liu, X., Li, J., Liu, L., Zhang, S., Du, W., Liu, S., Zhang, F., Li, J., Meng, J., and Wang,
 266 G.: Ammonia in urban atmosphere can be substantially reduced by vehicle emission control: A case study in
 267 Shanghai, China, J. Environ. Sci., 126, 754-760, 10.1016/j.jes.2022.04.043, 2023.

268 Wu, C., Wang, G., Li, J., Li, J., Cao, C., Ge, S., Xie, Y., Chen, J., Li, X., Xue, G., Wang, X., Zhao, Z., and Cao, F.:
 269 The characteristics of atmospheric brown carbon in Xi'an, inland China: sources, size distributions and optical
 270 properties, Atmos. Chem. Phys., 20, 2017-2030, 10.5194/acp-20-2017-2020, 2020b.

271 Wu, G., Wan, X., Ram, K., Li, P., Liu, B., Yin, Y., Fu, P., Loewen, M., Gao, S., Kang, S., Kawamura, K., Wang, Y.,
 272 and Cong, Z.: Light absorption, fluorescence properties and sources of brown carbon aerosols in the
 273 Southeast Tibetan Plateau, Environ. Pollut., 257, 10.1016/j.envpol.2019.113616, 2020c.

274 Xie, M., Chen, X., Holder, A. L., Hays, M. D., Lewandowski, M., Offenberg, J. H., Kleindienst, T. E., Jaoui, M.,
 275 and Hannigan, M. P.: Light absorption of organic carbon and its sources at a southeastern US location in
 276 summer, Environ. Pollut., 244, 38-46, 10.1016/j.envpol.2018.09.125, 2019.

277 Yao, X., Ling, T. Y., Fang, M., and Chan, C. K.: Comparison of thermodynamic predictions for in situ pH in
 278 PM_{2.5}, Atmos. Environ., 40, 2835-2844, 10.1016/j.atmosenv.2006.01.006, 2006.

279 Zhang, Y., Xu, J., Shi, J., Xie, C., Ge, X., Wang, J., Kang, S., and Zhang, Q.: Light absorption by water-soluble
 280 organic carbon in atmospheric fine particles in the central Tibetan Plateau, Environmental Science and
 281 Pollution Research, 24, 21386-21397, 10.1007/s11356-017-9688-8, 2017.

282 Zhao, Y., Wu, C., Wang, Y.-q., Chen, Y.-b., Lu, S.-j., Wang, F.-l., Du, W., Liu, S.-j., Ding, Z.-j., and Wang, G.-h.:
 283 Pollution Characteristics and Sources of Wintertime Atmospheric Brown Carbon at a Background Site of the
 284 Yangtze River Delta Region in China, Huanjing Kexue, 42, 3127-3135, 10.13227/j.hjcx.202012002, 2021.

285 Zhu, C.-S., Cao, J.-J., Huang, R.-J., Shen, Z.-X., Wang, Q.-Y., and Zhang, N.-N.: Light absorption properties of
 286 brown carbon over the southeastern Tibetan Plateau, Sci. Total Environ., 625, 246-251,

287 10.1016/j.scitotenv.2017.12.183, 2018.
288 Zou, C., Cao, T., Li, M., Song, J., Jiang, B., Jia, W., Li, J., Ding, X., Yu, Z., Zhang, G., and Peng, P. a.:
289 Measurement report: Changes in light absorption and molecular composition of water-soluble humic-like
290 substances during a winter haze bloom-decay process in Guangzhou, China, *Atmos. Chem. Phys.*, 23, 963-979,
291 10.5194/acp-23-963-2023, 2023.
292